

Control of Population Flow in Coherently Driven Quantum Ladders

Ruth Garcia-Fernandez,¹ Aigars Ekers,² Leonid P. Yatsenko,³ Nikolay V. Vitanov,^{4,*} and Klaas Bergmann¹

¹Fachbereich Physik der Universität, Erwin-Schrödinger-Strasse, 67653 Kaiserslautern, Germany

²Institute of Atomic Physics and Spectroscopy, University of Latvia, Raina Boulevard 19, LV-1586 Riga, Latvia

³Institute of Physics, National Academy of Science of Ukraine, prospect Nauki 46, Kiev-39, 03650, Ukraine

⁴Department of Physics, Sofia University, James Bourchier 5 Boulevard, 1164 Sofia, Bulgaria

(Received 15 March 2005; published 21 July 2005)

A technique for adiabatic control of the population flow through a preselected decaying excited level in a three-level quantum ladder is presented. The population flow through the intermediate or upper level is controlled efficiently and robustly by varying the pulse delay between a pair of partly overlapping coherent laser pulses. The technique is analyzed theoretically and demonstrated in an experiment with Na₂ molecules.

DOI: 10.1103/PhysRevLett.95.043001

PACS numbers: 32.80.Bx, 34.70.+e, 42.50.Vk

Laser control of quantum dynamics has become a standard tool in modern atomic, molecular, and optical physics [1]. Coherent light delivers numerous advantages compared to incoherent light, such as the possibility for complete population transfer between discrete levels, and it often shows intriguing counterintuitive features [2].

In this Letter, we analyze theoretically and demonstrate experimentally a technique for efficient control of the population flow through the upper state of a ladder of quantum levels by means of suitably delayed coherent laser pulses. The ladder consists of a nondecaying initial level 1 and rapidly decaying intermediate and upper levels 2 and 3. Each pair of levels is coupled by a laser pulse: P (primary) for the $1 \leftrightarrow 2$ transition and S (secondary) for $2 \leftrightarrow 3$, with two-photon resonance maintained between levels 1 and 3, as shown in Fig. 1. Variation of the pulse timing, with some overlap between the pulses, allows control of the course of the population flow out of the ladder. Obviously, if the P pulse arrives before the S pulse, the population loss occurs primarily through level 2 and little population reaches level 3. If the two pulses are applied simultaneously, some population reaches level 3 (due to population trapping [3]) and decays from there. If the pulses are applied counterintuitively, S before P , almost the entire population decays through level 3. The ability to control the flow through the highest level in a ladder will allow new experiments in collision dynamics between excited species or may enhance the efficiency when, for instance, the sensitivity of detection by laser induced fluorescence should be maximized or the excitation to a high Rydberg level is followed by field ionization.

This process is reminiscent of but *different* from stimulated Raman adiabatic passage (STIRAP) [2,4], which is a technique for complete and robust population transfer between *stable* quantum levels, usually implemented in Λ systems, where level 3 is long living. STIRAP can be implemented without conceptual difficulties in ladder systems if the pulse duration is shorter than the lifetime of level 3. STIRAP in a ladder system has already been

observed experimentally with nanosecond pulses in rubidium atoms [5]. In molecular ladders, STIRAP has been discussed [6] but not demonstrated yet.

We demonstrate here a STIRAP-like process in a ladder of rovibrational levels of Na₂ molecules when the lifetimes of levels 2 and 3 (12.5 and 17 ns) are much shorter than the interaction duration (~ 100 ns). We consider the population *flow* through these levels, as represented by the time-integrated populations, rather than the population transfer (which is ultimately zero). Maximizing the population flow through some excited molecular level is important in collision dynamics, especially for the control of branching of fragmentation. The technique presented here allows the preparation of atoms and molecules in highly excited states. Compared to excitation by chirped pulses, it leads to a higher efficiency since losses from the intermediate level are prevented. Compared to two-step excitation with frequencies detuned from resonance with the intermediate level, our approach requires significantly lower laser intensities. Furthermore, it is robust against moderate variations of intensity.

An essential difference from STIRAP is that in the present technique there is *no proper trapped state* since level 3 decays. A STIRAP-like population transfer to a lossy atom-cavity state has been demonstrated in a cavity

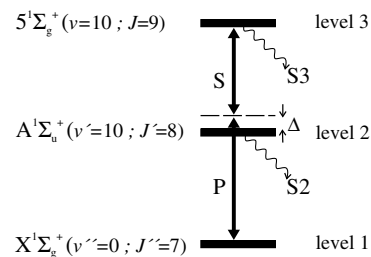


FIG. 1. The three-level ladder system. The initial and intermediate levels 1 and 2 are coupled by the P laser pulse, and level 2 and the final level 3 are coupled by the S pulse. The direct transition between levels 1 and 3 is dipole forbidden.

experiment, where the cavity provides the Stokes field, as a means of producing single photons on demand [7].

Another difference from STIRAP is that only the timing of the arrival of the pulses is important. In STIRAP the S pulse must arrive before the P pulse and must vanish first. Here the S pulse must also arrive first, but once the P pulse arrives, the population is quickly driven out of the ladder through level 3. The subsequent time dependence of the intensity is irrelevant as no population is left in the system.

A simplified diagram of the three-level ladder system in Na_2 is shown in Fig. 1. As for STIRAP, we require two-photon resonance between levels 1 and 3, while level 2 may be off resonance by a certain detuning Δ . A detailed theoretical analysis of the population flow control will be presented elsewhere [8]. Here we discuss the most significant theoretical conclusions.

If we neglect spontaneous emission *within* the system ($3 \rightarrow 2$ and $2 \rightarrow 1$), the quantum dynamics of the ladder system is described by the Schrödinger equation [1],

$$i\hbar \frac{d}{dt} \mathbf{c}(t) = \mathbf{H}(t) \mathbf{c}(t), \quad (1)$$

where the Hamiltonian in the rotating-wave approximation is given by [2,4]

$$\mathbf{H}(t) = \frac{\hbar}{2} \begin{bmatrix} 0 & \Omega_p(t) & 0 \\ \Omega_p(t) & 2\Delta - i\Gamma_2 & \Omega_s(t) \\ 0 & \Omega_s(t) & -i\Gamma_3 \end{bmatrix}. \quad (2)$$

Here the column vector $\mathbf{c}(t) = [c_1(t), c_2(t), c_3(t)]^T$ comprises the probability amplitudes of the three levels, and the respective populations are $P_n(t) = |c_n(t)|^2$ ($n = 1, 2, 3$). The functions $\Omega_p(t)$ and $\Omega_s(t)$ represent the Rabi frequencies of the P and S pulses, respectively: $\Omega_p(t) = -\mathbf{d}_{12} \cdot \mathbf{E}_p(t)/\hbar$ and $\Omega_s(t) = -\mathbf{d}_{23} \cdot \mathbf{E}_s(t)/\hbar$, where $\mathbf{E}_{p,s}(t)$ is the respective laser electric-field amplitude and \mathbf{d}_{mn} is the corresponding transition dipole moment. The decay rates Γ_2 and Γ_3 describe the irreversible population losses, which occur from levels 2 and 3 primarily by spontaneous emission to other levels outside the system. We measure the fluorescence signals from levels 2 and 3,

$$S_n = \int_{-\infty}^{\infty} \Gamma_n P_n(t) dt \quad (n = 2, 3). \quad (3)$$

In the absence of decay, we have a STIRAP process that proceeds through the trapped state,

$$|\phi_0(t)\rangle = \frac{\Omega_s(t)|1\rangle - \Omega_p(t)|3\rangle}{\Omega(t)}, \quad (4)$$

where $\Omega(t) = \sqrt{\Omega_p^2(t) + \Omega_s^2(t)}$. The trapped state (4) is an eigenstate (adiabatic state) of the Hamiltonian (2) for $\Gamma_2 = \Gamma_3 = 0$, with a zero eigenvalue. When the S pulse precedes the P pulse (counterintuitive order), the trapped state $|\phi_0(t)\rangle$ is equal to state $|1\rangle$ as $t \rightarrow -\infty$ and to state $-|3\rangle$ as $t \rightarrow \infty$. For adiabatic evolution, which requires large

pulse areas [4], the population remains trapped in state $|\phi_0(t)\rangle$ at all times and ends up in level 3. Moreover, the intermediate level 2 does not receive any population because state $|\phi_0(t)\rangle$ does not involve it.

In the presence of decay, essential differences with STIRAP emerge. First of all, state $|\phi_0(t)\rangle$ is not trapped because if Γ_2 and Γ_3 are not zero, this state is coupled to the other adiabatic states, with subsequent population losses. For strong decay ($\Gamma_2, \Gamma_3 \gg T^{-1}$, where T is the pulse duration), as in our experiment, these decay-induced couplings are larger than the nonadiabatic couplings caused by the time dependence of the Hamiltonian and lead to population losses to the other two adiabatic states; hence larger pulse areas are needed to maintain adiabaticity. For strong decay, the adiabatic condition on and far-off single-photon resonance reads [8]

$$\Gamma_3 \sin 2\vartheta(t) \ll \sqrt{2}\Omega(t), \quad (\Delta = 0), \quad (5a)$$

$$\Gamma_3 \sin 2\vartheta(t) \ll \frac{\Omega^2(t)}{2\Delta}, \quad (|\Delta| \gg \Omega), \quad (5b)$$

where $\vartheta(t) = \tan^{-1}[\Omega_p(t)/\Omega_s(t)]$. Hence adiabaticity improves with Ω on resonance and with Ω^2 off resonance, and deteriorates as the decay rate Γ_3 and the detuning Δ increase. A more careful analysis of the population dynamics shows that for efficient population flow through level 3 it is necessary, besides the large-area condition $\Omega_{p,s}^{\max} T \gg 1$, that [8]

$$\Omega_s^2 \gg \Gamma_2 \Gamma_3, \quad (6)$$

during the relevant time interval, requiring $\Omega_s > 100$ MHz under the conditions of our experiment (with typical values of 400 MHz). This interval begins with the arrival of the P pulse and ends within $T_{\text{flow}} \simeq \Gamma_3^{-1} \ll T$. The late part of the interaction is irrelevant because by this time the population has decayed out of the ladder. This observation is in sharp contrast to STIRAP, where the S pulse must vanish first.

The case treated in this work is intermediate with regard to level 3 being a stable or a continuum state. When level 3 is stable, $\Gamma_3 T \sim 0$, the STIRAP process can be implemented with 100% *transfer* to the final state. Here we have $\Gamma_3 T \sim 10$, still allowing nearly complete *flow* through the final level. When level 3 is a continuum state, Eqs. (5) and (6) show that adiabatic transfer is no longer possible and an appreciable part of the population flows through the intermediate level.

These features are illustrated in Fig. 2, which shows the time evolutions of the numerically calculated populations and fluorescence signals. Although the pulse areas ($\sim 28\pi$) are sufficient for adiabatic evolution in STIRAP, here adiabaticity is imperfect and the intermediate-level population is small, but nonzero; consequently, some population decays through level 2. The population flow through level 3 is very high, and we have verified that it approaches unity as the pulse areas increase further. The

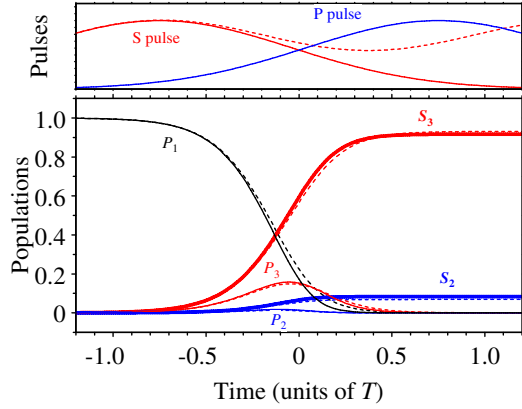


FIG. 2 (color online). Time evolutions of the numerically calculated populations $P_{1,2,3}$ and fluorescence signals $S_{2,3}$. The solid curves are for counterintuitively ordered Gaussian pulses: $\Omega_p(t) = \alpha_p e^{-(t+\tau/2)^2/T^2}$ and $\Omega_s(t) = \alpha_s e^{-(t-\tau/2)^2/T^2}$, with $\tau = -1.5T$, $\alpha_p = \alpha_s = 50T^{-1}$, and $\Gamma_2 = \Gamma_3 = 10T^{-1}$. The dashed curves are for the same P pulse, while the S pulse is $\Omega_s(t) = \alpha_s e^{-(t-\tau/2)^2/T^2} + \alpha_s e^{-(t+\tau/2)^2/T^2}$: it begins before and vanishes after the P pulse.

population dynamics ends shortly after the P pulse arrives; hence, the temporal behavior of the fields thereafter is irrelevant. We compare the typical pulse ordering in STIRAP, with the S pulse arriving first and vanishing first (solid curves) and the case when the S pulse arrives before and vanishes after the P pulse (dashed curves). The close similarity between solid and dashed curves in the lower part of Fig. 2 confirms that the timing of the trailing edges is irrelevant. In contrast, in STIRAP the population would return to the initial level 1 for the latter pulse timing.

Calculated contour plots of the signals from levels 2 and 3 vs pulse delay and the pulse area are shown in Fig. 3. The latter figure reveals that the pulse delay can be used as an efficient tool for directing the population flow through levels 2 or 3. For positive delay (PS order) and for large negative delay (no overlap) the population flows through level 2, while for moderate negative delay (SP order) it

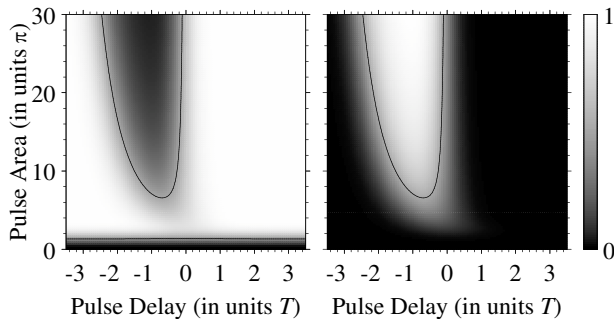


FIG. 3. Numerically calculated fluorescence signals S_2 (left) and S_3 (right) for Gaussian pulses against the pulse delay and the pulse area for decay rates $\Gamma_2 = \Gamma_3 = 10T^{-1}$. Dark areas show regions with little, if any, excitation. The excitation probability is 0.5 along the thin solid line.

flows through level 3. As the pulse areas increase, adiabaticity improves and these features strengthen.

The experiments were performed in a collimated supersonic beam of Na_2 molecules, with mean longitudinal velocity of 1340 m/s and velocity spread of 260 m/s. The beam diameter was 3 mm, with a divergence angle of 1° , resulting in a transverse Doppler width of 30 MHz. About 99% of the molecules were in the ground vibrational level $v'' = 0$, with the rotational-level distribution peaking at $J'' = 7$. The molecular beam was crossed by three parallel cw laser beams (all Coherent Co., CR-699-21 dye lasers, with linewidth $\Delta\nu_L = 1$ MHz) at right angles. The P and S laser beams were polarized parallel to the molecular beam axis. Fluorescence from the interaction zone was collected by two optical fiber bundles and detected by two photomultipliers equipped with filters to separate the fluorescence from levels 2 and 3. The detection laser beam crossed the molecular beam further downstream, and its frequency was tuned to resonance of the $v'' = 1$, $J'' = 11$ level of the electronic ground state with some rovibronic level in the $A^1\Sigma_u^+$ level, and the fluorescence from the excited level was detected. Since the former level was populated exclusively through cascading after the excitation of level 3, and it was not collisionally depleted under the supersonic beam conditions, the fluorescence induced by the detection laser provided a direct measure of population flow through level 3. The population flow can be normalized when the corresponding electronic and rovibronic branching coefficients are known. The population in rovibrational levels of the $5^1\Sigma_g^+$ state decays primarily to the states $A^1\Sigma_u^+$, $B^1\Pi_u$, and $2^1\Sigma_u^+$, and to a lesser extent to $3^1\Sigma_u^+$ and $2^1\Pi_u$. Together with the corresponding Franck-Condon and Hoenl-London factors, we find that the main contribution to the population of level ($v'' = 1$, $J'' = 11$) is due to the decay via the state $A^1\Sigma_u^+$; only about 20% of the population of level 3 decay to level 2. A detailed discussion of the normalization will be presented elsewhere [9].

The P and S laser beams were focused onto the molecular beam using cylindrical lenses to a Gaussian waist of $140 \mu\text{m}$, with the long axis of $1150 \mu\text{m}$ aligned perpendicular to the molecular beam axis. The focal position of the P beam with respect to that of the S beam was variable along the molecular beam axis. The positioning was controlled by a stepper motor, and the beam waists and their displacements were measured and calibrated using the beam profile measurement device Dataray Beamscope P7 (resolution $4 \mu\text{m}$). We used the signal induced by the detection laser to verify that the fluorescence signal from level 3 collected from the interaction zone is free from possible distortions due to the displacement of the P laser beam.

Figure 4 shows the fluorescence signal from level 3 as a function of displacement between the P and S fields for two values of the single-photon detuning: $\Delta = 0$ MHz

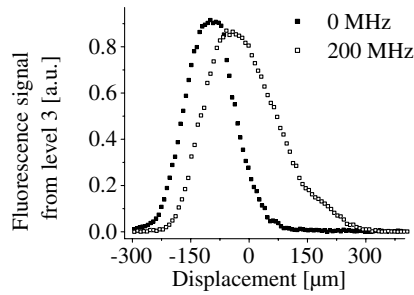


FIG. 4. Fluorescence signal from level 3 against the displacement between the P and S laser beams for two values of the single-photon detuning Δ : 0 (resonance) and 200 MHz. Two-photon resonance ($\delta = 0$) is maintained. Negative (positive) displacement corresponds to the $S(P)$ beam coming first.

(resonance) and $\Delta = 200$ MHz, while two-photon resonance is maintained in both cases. A strong increase of the signal from level 3 is observed for negative displacement, when the molecules interact with the S field first. Three features are clearly observed. First, the maximum signal is almost unaffected by the detuning; this robustness is expected because nearly adiabatic conditions are maintained. Second, for $\Delta = 200$ MHz the maximum of the signal shifts towards smaller pulse delays (beam displacements). As stated above [see Eq. (5b)], the detuning hinders adiabaticity: its effect is more pronounced when adiabaticity is imperfect (i.e., for larger negative displacements), and it reduces the signal there, as seen in Fig. 4. Third, for $\Delta = 200$ MHz the signal S_3 increases considerably closer to zero displacement (full overlap). This increase occurs because the detuning Δ reduces the population flow through level 2; consequently, more population can reach level 3 via direct two-photon excitation, and decay through it.

Figure 5 shows the fluorescence signal from level 3 as a function of the beam displacement in the case when the intensity of one of the beams is fixed and the other varies. As the respective intensity increases, the signal also increases, indicating improved adiabaticity, as follows from Eq. (5). For sufficiently high intensities the signal saturates, which demonstrates robustness against intensity variations. As the intensity of the P laser increases (upper frame), the maximum of the signal moves towards larger beam displacements, whereas it barely changes when the S laser intensity increases (lower frame). The shift for fixed S intensity can be explained by the fact that for weaker P pulse the rate of change of population is smaller and thus the transfer process lasts longer and ends later; then for the S field to be large enough during the period when the transfer occurs, the delay between P and S pulses must be shorter. In contrast, for fixed P intensity the duration of the transfer process is also fixed and the timing of the S pulse is not important, as long as there is sufficient overlap:

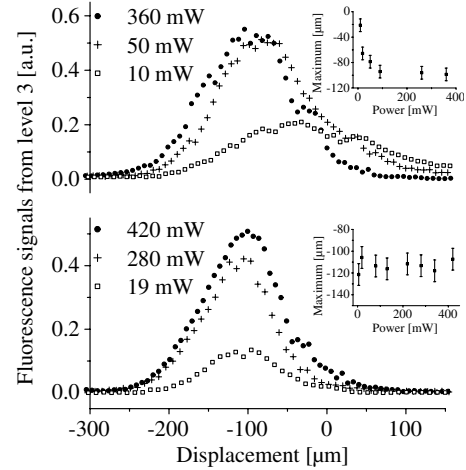


FIG. 5. Fluorescence signals from level 3 against the displacement between the P and S laser beams. Negative (positive) displacement corresponds to $S(P)$ beam coming first. Upper frame: S intensity is fixed at 420 mW, various P intensities (denoted). Lower frame: P intensity is fixed at 320 mW, various S intensities. The insets show the position of the maximum of the signal vs the intensity of the respective laser.

increasing the S power simply improves adiabaticity and increases the signal.

In conclusion, we have demonstrated an efficient and robust adiabatic technique that allows the control of the course of population flow out of a molecular ladder through a selected decaying level by means of the delay between two pulsed laser fields.

This work was supported by the EU RTN project QUACS, the EU TOK projects LAMOL and CAMEL, Max-Planck Forschungspreis 2003 (K. B.), INTAS Grant No. 2001-0155, Deutsche Forschungsgemeinschaft, and by the European Social Fund, Latvian Science Council, and NATO Grant EAP.RIG.981387 (A. E.).

*Also at Institute of Solid State Physics, Bulgarian Academy of Sciences, 1784 Sofia, Bulgaria.

- [1] B. W. Shore, *The Theory of Coherent Atomic Excitation* (Wiley, New York, 1990).
- [2] N. V. Vitanov *et al.*, *Annu. Rev. Phys. Chem.* **52**, 763 (2001).
- [3] E. Arimondo, in *Progress in Optics* (North-Holland, Amsterdam, 1996), Vol. XXXV, pp 259–356.
- [4] N. V. Vitanov *et al.*, *Adv. At. Mol. Opt. Phys.* **46**, 55 (2001).
- [5] W. Süptitz *et al.*, *J. Opt. Soc. Am. B* **14**, 1001 (1997).
- [6] M.-L. Almazor *et al.*, *Eur. Phys. J. D* **5**, 237 (1999).
- [7] M. Hennrich *et al.*, *Phys. Rev. Lett.* **85**, 4872 (2000).
- [8] L. P. Yatsenko *et al.* (to be published).
- [9] R. Garcia-Fernandez *et al.* (to be published).